Indonesian Journal of Electrical Engineering and Informatics (IJEEI)
Vol. 10, No. 2, June 2022, pp. 246~262
ISSN: 2089-3272, DOI: 10.52549/ijeei.v10i2.3700

Novel design and simulation of fuzzy controller for turn-on & turn-off angle in coordination with SRM speed control for electric vehicles

M Naveen Kumar[1], R Chidanandappa[2]
[1,2]Department of Electrical and Electronics Engineering, The National Institute of Engineering, Mysuru, Karnataka, India

Article Info

Article history:

Received Jan 31, 2022
Revised Apr 6, 2022
Accepted Apr 19, 2022

Keyword:

Switched Reluctance Motor (SRM)
Integral Absolute Error (IAE)
Integral Square Error (ISE)
Integral Time Absolute Error (ITAE)

ABSTRACT

In current scenario, the Switch Reluctance Motor (SRM) are powerful alternative for Electric vehicles applications, due to its simple and rugged structure, high speed, its fault tolerance ability and Magnet-free design these attributes make SRM superior to other conventional machines. This motor is a reluctance torque-driven stepper motor that can be used for bi-directional control and self-starting applications. In This paper, novel control strategy proposed is to minimizing the Multiobjective function for accurate speed control of SRM by using Mamdani-based two-input two output fuzzy controller for optimal evaluation of α and β-angle by designing closed loop system for accurate speed control of SRM and the corresponding error indices ITAE, IAE, ISE for with and without controller is analyzed and compared modelling and simulation is done using MATLAB 2020a.

Corresponding Author:

M Naveen Kumar
Department of Electrical and Electronics Engineering,
The National Institute of Engineering
Mysuru, Karnataka-570008, India.
mudavathnaveen94@gmail.com

1. INTRODUCTION

The design of Electric Vehicles (EVs) and hybrid EVs have grown in popularity as a result of the increased demand for environmental protection against air pollution and fuel efficiency [1]. Minimization of volume and energy loss of high-speed Permanent Magnet Synchronous Motors (PMSMs) for electric and hybrid vehicle applications is discussed in [2]. Self-sensing control schemes and stability issues of PMSM are discussed in [3]. The drawback of PMSM is rare earth materials usage is higher compared to SRM. Because of their rare-earth-free nature and outstanding performance of Switched reluctance motors have received much interest from both industry and academia [4]. It is a stepper motor that works with a reluctance torque. The SRM has a position sensor that detects the stator's energized pole and aligns the rotor with it [5]. It provides improved controllability, engine speed and bi-directional control. It is the ideal choice for high-speed variable speed drives because it has no coil or magnet on the rotor [6]. The various advantages of SRM such as their strength, simplicity and ease of maintenance, as well as their low cost, with increased fault tolerance and the ability to handle a wide range of loads, the lack of permanent magnets and copper coils in the rotor and the speed range in constant power, make it a suitable serious contender and reliable for use in industry, particularly in the automotive industry [7-8].

The main drawbacks of SRM include low efficiency, torque ripple, temperature rise, noise, and overall cost, all of which can be reduced by using static and dynamic system-level simulations and finite element analysis [9]. A low torque ripple is required when using an SRM in a high-power application [10]. For advanced control mechanisms, the first step is to improve mechanical design, and the second is to apply an electrical implementation approach. Only through altering mechanical design features such as stator and

rotor pole structures at the expense of motor performance is feasible to improve. Because of their inherent fault-resilient nature, SRM drive systems have become more reliable in recent years than other machine drive systems. As a result, a malfunction in one phase has no influence on the other phases, although tolerance features are not present in other machine drive systems such as induction motor drives [11].

The SRM's characteristics must be considered in the control technique. The nonlinear electromechanical behavior which can be achieved by carefully selecting various operational parameters such as α and β angles, voltage, current, and shaft load [12]. By using Propositional integral (PI) controller MPPT design-based PV system supplied power to SRM, because of PI controller MPPT exact tracking of maximum power point is not obtained; due to this an BAT optimization algorithms is used and compared it with a Particle swarm optimization (PSO) [13]. Because of their simple form, these motors do not require the use of expensive materials and their production is more cost effective. Variable speed motors are used in a variety of applications, including aviation power systems (owing to their great reliability), pump gas turbines, wind generators, and electric cars [14]. The SRM has various advantages over conventional motors including a magnet-free, proper rotor construction that enables for high-speed operation. For EV applications SRM is a potential traction machine solution. In hybrid electric vehicles SRM outperforms induction motors and permanent magnet motors [15].

Minimization of High torque ripples of SRM low torque/power density [16]. 8/6 solid rotor SRM is designed for working in water environment in nuclear reactors. Here two-phase excitation method is presented for rotor position estimation, for better rotor position estimation ANN structures are trained. For this approach, less voltage and current sensors are used [17]. When addressing the needs of traction applications, torque ripple minimization is one of the most significant and hardest SRM design components. Torque ripples were eliminated using two strategies: structural design and improved SRM control technologies [18]. To further reduce torque ripples of the SRM multi-stack and multi-layer structures were introduced in [19]. Proton exchange membrane fuel cells (PEMFC) are a source, optimization and operating performance of SRM. A multi-objective dragonfly approach (MODA) was used for optimal generation of alpha(α) and beta (β) angles of bridge converters and gains of a PI speed controller for different load torques [20]. The Switched Reluctance motor has a better cooling system than conventional motors because the rotor has no winding. It has a high fault tolerance; thus, it can operate 24/7, which is best suited for large industries [21]. Using sliding mode and feedback linearization controllers designed for accurate speed regulation of SRM is presented and analyzed in [22]. Non -Dominated Sorting Genetic Algorithm (NSGA) is used to offer a control mechanism for speed regulation of SRM with torque ripple reduction. Here the control mechanism includes a PI speed control in the outer loop and a PI current controller in the inner loop, as well as constant alpha and beta are used [23]. Fuzzy logic-based Beta (β) compensation for torque ripple reduction is demonstrated in SRM. The Beta-angle is automatically changed as a sophisticated function of motor speed and current throughout a wide motor speed range to prevent ripple in SRM is presented and discussed in [24].

Many optimizations liaison (MOL) algorithms speed control of SRM and torque ripple reduction with constant α and β angle are described in [25]. Speed control of SRM is discussed by using PI controller with constant α and β and it will take more time to settle its rated speed [26]. The torque ripple effect of SRM is reduced by using artificial neural networks with constant angles (α, β) in this method, rated speeds can settle with less time [27]. The effectiveness of SRM as well as various speed control techniques such as PI and fuzzy are reviewed in [28]. Particle-swam optimization algorithms (PSO) speed control of SRM can be designed and analyzed and are also more concentrated on minimization of integral square error indices [29]. Ant colony optimization (ACO) algorithm is used for speed control of SRM and PV source is used for this proposed method. The ACO algorithm was compared with genetic algorithm-based PV controllers for better speed control of SRM [30].

From the literature review above, speed control of SRM and Torque ripple is minimized, but it is for only constant α and β angle. But in this proposed work, work has been carried out by taking into account precise tuning of α and β using Mamdani-based Two-input Two-output-based fuzzy controllers.

2. MODELLING OF PLUG IN ELECTRIC VEHICLE

Plug-in electric vehicle (PEV) are the eco-friendly electric vehicles which use electricity as the main source of energy to drive the electric motor. The PEV compose of AC-DC, Power factor correction circuit, DC-DC Converter, Bidirectional Converter, electric motor and battery management system. The base principal of power flow takes place from source to motor via power converter based on the turn-on and turn-off angle of the power converter. For accurate speed control of PEV the SRM is used as speed driver with fuzzy logic controller.

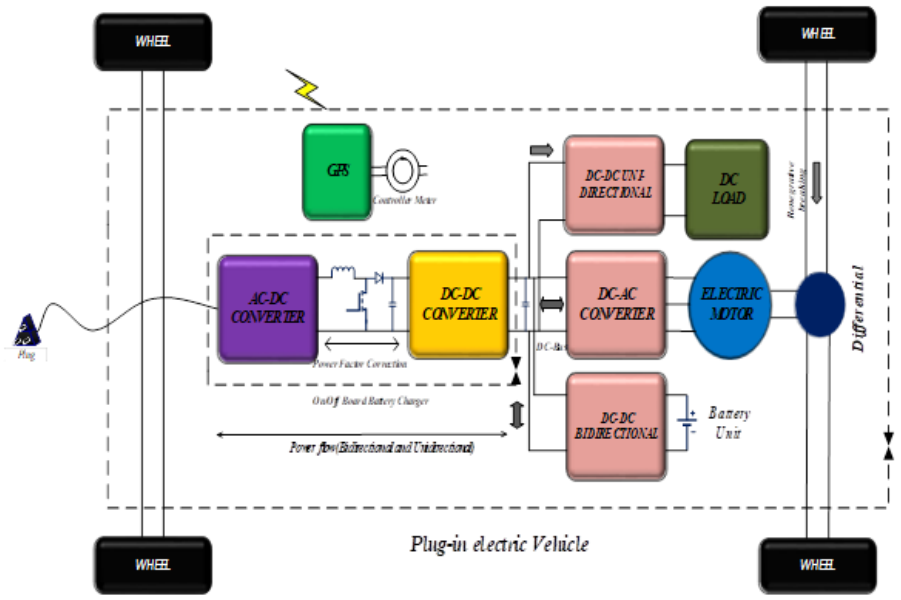

Figure 1. Modelling of Plug in Electric Vehicle

3. POWER EQUATION OF SRM

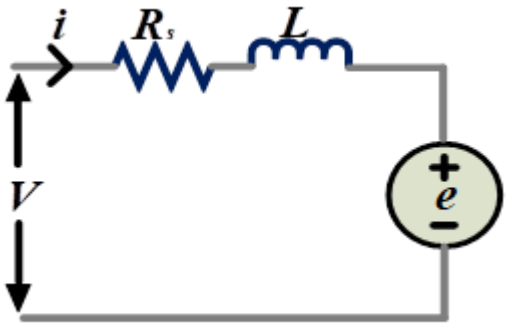

Figure 2. Single phase equivalent circuit of SRM

Figure 2 shows the Single-Phase equivalent circuit of an SRM Drive. As a simplification, we will ignore the mutual inductance between the phases in the circuit below [31].

The Phase Voltage (V_{phase}) is defined as the sum of the resistive voltage drop and the rate of flux connections.

$$V = R_s i + \frac{d\lambda(\phi,i)}{dt} \quad (1)$$

Where,
Rs= per-phase resistance,
λ= per-phase flux linkage
Equation of λ given by:

$$\lambda = L(\phi, i).i \quad (2)$$

Where,
L= inductance dependent on the position of the rotor and I_{Phase} .
Therefore, the V_{Phase} equation is

$$V = R_s i + \frac{d\{L(\phi,i)i\}}{dt} = R_s i + L(\phi,i)\frac{di}{dt} + i\frac{d\phi}{dt}.\frac{dL(\phi,i)}{d\phi}$$

$$V = R_s i + L(\phi,i)\frac{di}{dt} + \frac{dL(\phi,i)}{d\phi}\omega_m i \quad (3)$$

The induced emf(e) is obtained as:

$$e = \frac{dL(\phi,i)}{d\phi}\omega_m i = K_b \omega_m i \quad (4)$$

Where,
K_b = The emf constant is expressed here as and is similar to that of the DC machine:

$$K_b = \frac{dL(\phi,i)}{d\phi} \quad (5)$$

The emf constant is a function of the operating point and it is calculated using a constant current point. When the flux connections are substituted for in the voltage equation and the current is multiplied.
Then the instantaneous input power is provided by

$$P_i = V.i$$

$$P_i = R_s i^2 + i^2\frac{dL}{dt}(\phi,i) + L(\phi,i)i\frac{di}{dt} \quad (6)$$

The last term is physically uninterpretable in this case; nevertheless, it can be expressed in terms of known variables as follows:

$$\frac{d}{dt}\left(\frac{1}{2}L(\phi,i)i^2\right) = L(\phi,i)i\frac{di}{dt} + \frac{1}{2}i^2\frac{dL(\phi,i)}{dt} \quad (7)$$

Equation 7 is substitute in equation 6

$$P_i = R_s i^2 + \frac{d}{dt}\left(\frac{1}{2}L(\phi,i)i^2\right) + \frac{1}{2}i^2\frac{dL(\phi,i)}{dt} \quad (8)$$

The input power at any given time is denoted by P_i. The P_i is the total of the winding resistive losses given by $R_s i^2$the rate at which the field energy changes, defined by $p[i^2L(\theta,i)]i^2/2$, and the P_{airgap}, which is identified by the phase $[i^2pL(\theta,i)]/2$, in which p denotes the differential operator i.e., d/dt. In terms of speed and rotor position, time is substituted by

$$t = \frac{\phi}{\omega_m} \quad (9)$$

When power is applied to the air gap, it produces

$$P_a = \frac{1}{2}i^2\frac{dL(\phi,i)}{dt} = \frac{1}{2}i^2\frac{dL(\phi,i)}{d\phi}.\frac{d\phi}{dt} = \frac{1}{2}i^2\frac{dL(\phi,i)}{d\phi}\omega_m \quad (10)$$

The electromagnetic torque and rotor speed are multiplied to
get the air gap power

$$P_a = \omega_m T_e \quad (11)$$

By equating equation 10 and 11, we will get Electromagnetic Torque

$$T_e = \frac{1}{2}i^2\frac{dL(\phi,i)}{d\phi} \quad (12)$$

4. PROPOSED METHODOLOGY

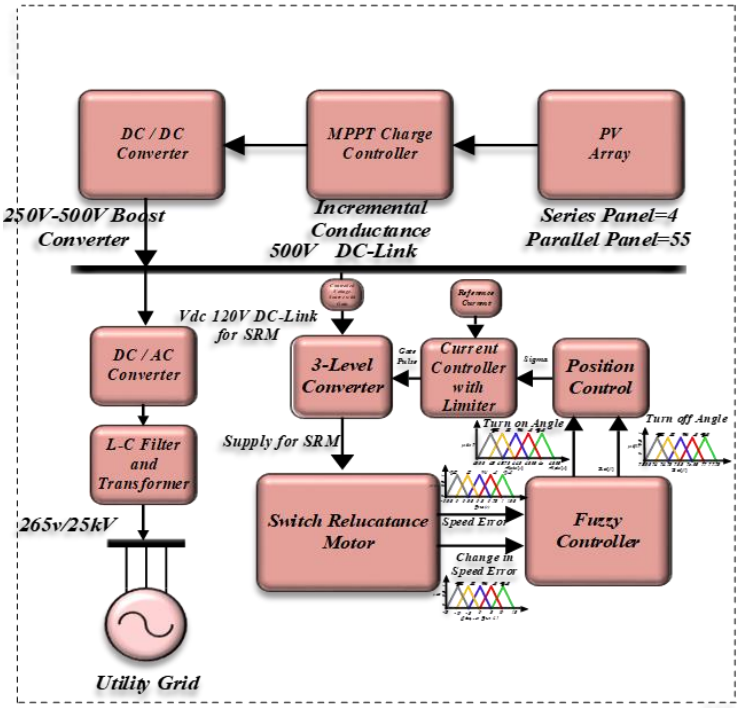

Figure 3. Proposed Fuzzy based SRM speed Controller

In the proposed system shown in figure 3 it consists of a 60kW solar plant feeding power to the grid and SRM; in our system the grid acts like a swing bus so the net power is fed to the SRM. If additional load is added to the system, then the power has been received from the swing bus. Solar PV array consists of 50 parallel string and 4 series string to get maximum power of 60.137kW and MPPT, voltage and current rating of 215.042V and 279.655 A for short circuit current and open circuit voltage of 298.92A 253.29V for fixed irradiance and temperature of 1000w/m2 and 30°C, respectively. MPPT charge controllers work based on the incremental conductance technique; the converter is operated at a duty cycle of 0.5, so that the output voltage of DC-Link is 500V.The DC link is used as a supply for the inverter which generates 265V AC after L-C filtering, then the AC voltage is stepped up to utility voltage of 25kV.

The DC-link voltage is fed to 3 level Converter through Controlled voltage regulator in DC mode. SRM DC link is 120V which is fed from the controlled voltage regulator. Mamdani based Fuzzy controller is designed for regulating α and β angle of SRM. Closed loop control design for SRM motor speed control is based on the feedback signal of speed error and change in speed error which is two inputs for fuzzy controller and that fuzzy controller give α and β angle from that position sensor is used to calculate the sigma angle which is used to generated the actual current which is compared with reference current then that error current signal is pass to limiter to generate the clock pulse for three level Inverter to power the SRM. Tuning of alpha and beta is essential for speed control of SRM detail design of fuzzy logic design is given in fuzzy controller design.

4.1. Multi-Objective function

A multi-objective function is defined as follows

$$f_0 = f_{\min}(f_1 + f_2 + f_3) \tag{13}$$

$$f_1 = IAE = \int_0^{\infty} |e_\omega| dt \tag{14}$$

$$f_2 = ITAE = \int_0^{\infty} t.|e_\omega| dt \tag{15}$$

$$f_3 = ISE = \int_0^{\infty} e_{\omega}^2 \, dt \quad (16)$$

Where,

$e_{\omega} = \omega_{ref_{p.u}} - \omega_{act_{p.u}}$

e_{ω} is the speed error in per unit

$\omega_{ref_{p.u}}$ reference speed in per unit i.e., is 1 p.u

$\omega_{act_{p.u}}$ actual speed in per unit

4.2. Flow Chart for Proposed System

Figure 4 Shows Flow Chart for Proposed System; this flow chart gives the overall evaluation of SRM speed control with minimization of multi objective function; the steps are as follows.

1. Read the data from the test system i.e., 60kw solar power plant obtain its system parameters such as Solar PV-IV characteristics and evaluate the DC-DC boost converter voltage.
2. Feed boost converter output to SRM via Controlled Voltage source and 3-Level Inverter.
3. Define objective function
4. Measure the speed of SRM and evaluate Error indices. IAE, ITAE and ISE. Save these results as base case (Without Controller).
5. If objective function is not satisfied without controller, then evaluate the objective function Via two input two output fuzzy controller, until objective function minimization.
6. Print results.

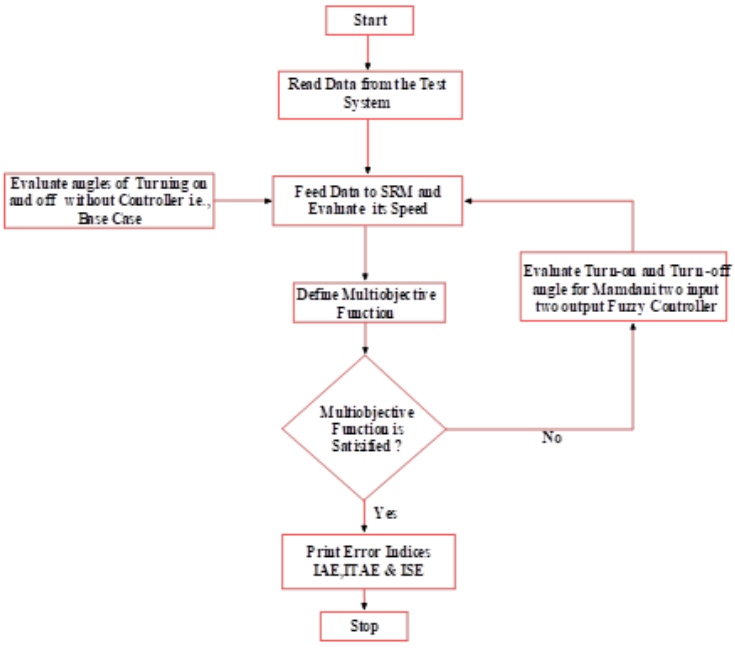

Figure 4. Flow Chart for Proposed System

5. Fuzzy Controller detail design for Proposed System

Fuzzy logic can be applied to systems where human constraints are met by fuzzy. Firstly, a basic understanding of fuzzy is essential, in figure 5; Single triangular membership function 'A' present in the interval of $x1$, $x2$ and $x3$ the value of membership function at x is given by $\mu_A(x)$

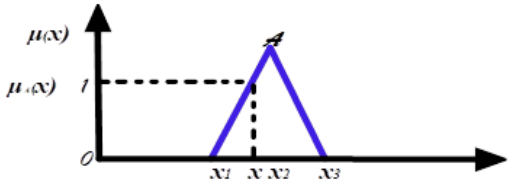

Figure 5. Single Triangular Membership function

$$\mu_A(x) = \begin{cases} \dfrac{|x| - |x_1|}{|x_2| - |x_1|}, & for\ x_1 \le x \le x_2 \\ \dfrac{|x_1| - |x|}{|x_3| - |x_2|}, & for\ x_2 \le x \le x_3 \\ 0, & otherwise \end{cases}$$

$$\mu_A(x) = max\left(min\left(\frac{x - x_1}{x_2 - x_1}, \frac{x_3 - x}{x_3 - x_2}\right), 0\right)$$

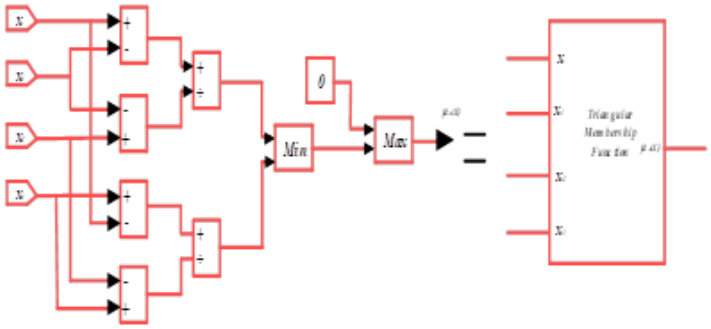

Figure 6. Block Diagram of single triangular membership function

In figure 6, where we can see the detail diagram inside the fuzzy controller for single membership functions, it's a mathematical block diagram based on the function $\mu_A(x)$. So, for five membership functions, figure 6 has been connected in parallel.

In our design we have used a triangular membership function for both the input and output of the fuzzy controller.

Input 1: Speed Error
Partition of speed error into 5 subsets {VS, S, M, L, VL}
Parameter range {-0.25 to 1.25}

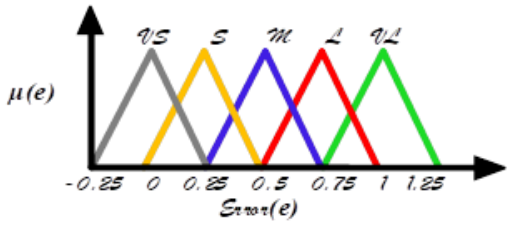

Figure 7. Speed Error as Input1 Membership function

Input 2: Change in Speed Error
Partition of change in speed error into 5 subsets {VS, S, M, L, VL}
Parameter range {-15 to 15}

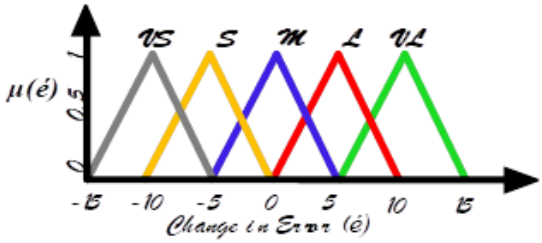

Figure 8. Change in Speed Error as Input2 Membership function

Output 1: Turn-on Angle (α)
Partition of speed error into 5 subsets {VS, S, M, L, VL}
Parameter range {42.25 to 45.25}

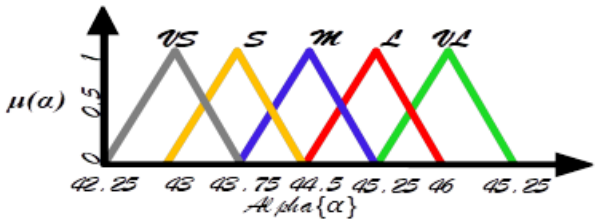

Figure 9. Turn-on Angle as Output 1 Membership function

Output 2: Turn-off Angle (β)
Partition of speed error into 5 subsets {VS, S, M, L, VL}
Parameter range {73.25 to 77.75}

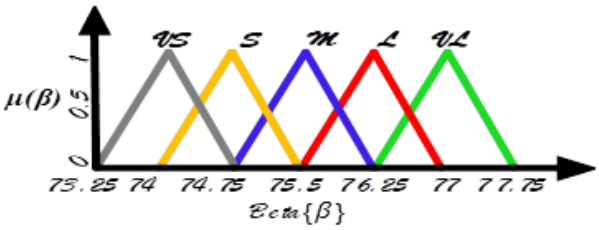

Figure 10. Turn-off Angle as Output 2 Membership function

5.1. Proposed Two Input Two Output Fuzzy Controller

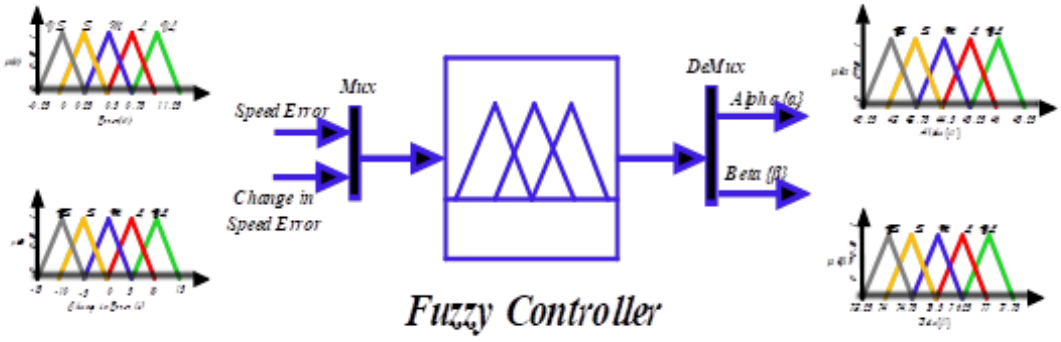

Figure 11. Full Structure of Proposed Fuzzy Controller

Figure 11 shows the full fuzzy structure of the proposed system; the proposed fuzzy controller is Mamdani two input, two output fuzzy controller, where the figures 7-8 are the input membership function and figures 9-10 are the output membership function. The fuzzy controller yields the accurate value of the turn-on and turn-off angle in coordination with speed error and change in speed error. Corresponding surf view as show in figure 12-13.

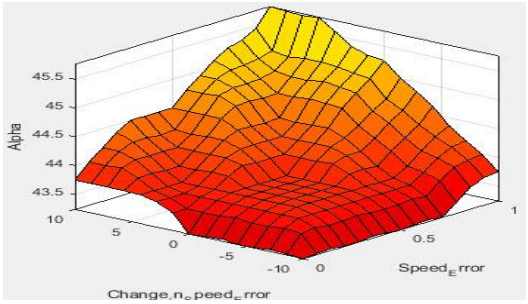

Figure 12. Alpha surf View

Table 1. Truth table (5x5) for Alpha Partition and its Surf View

Partition of Alpha(α) into five subsets					
$\frac{e}{\frac{de}{dt}}$	***VS***	***S***	***M***	***L***	***VL***
VS	*VS*	*VS*	*S*	*S*	*S*
S	*VS*	*S*	*S*	*M*	*M*
M	*VS*	*S*	*M*	*M*	*L*
L	*VS*	*S*	*M*	*L*	*L*
VL	*M*	*L*	*L*	*VL*	*VL*

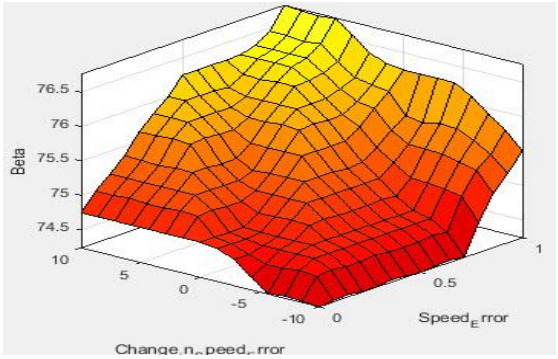

Figure 13. Beta Surf View

Table 2. Truth table (5x5) for Beta Partition and its Surf View

Partition of Alpha(α) into five subsets					
$\frac{e}{\frac{de}{dt}}$	***VS***	***S***	***M***	***L***	***VL***
VS	*VS*	*VS*	*VS*	*S*	*S*
S	*VS*	*S*	*S*	*S*	*M*
M	*VS*	*S*	*S*	*M*	*M*
L	*VS*	*S*	*M*	*M*	*L*
VL	*S*	*M*	*L*	*VL*	*VL*

6. SIMULATION MODEL OF SRM DRIVE AND RESULTS

Simulink model of PV system integration with Grid as shown in figure 14 here for fixed irradiation and temperature power output of PV system is obtained and corresponding characteristic of PV system is shown in figure 18. The generated PV power output is tracked with MPPT Charge controller and it's feed to boost converter with the duty cycle 50%. Consequently, the DC-link will be 2 times the input of the boost converter. 500V DC-link is used as used to energise the SRM controller via controlled voltage source SRM motor is 120V rating therefore the gain is 120/500 (V_{motor}/V_{DC}), this signal has been injected to a controlled voltage source which develops the DC voltage for SRM and the three-level converter is used to drive the balance power to SRM. For motor operation the gain of k_{motor} is 0 for generator mode it should be -1. This parameter is the torque load of this machine. The corresponding flux, current, torque and speed are measured corresponding Simulink model is illustrated in figure 15.

Modelling of Closed Loop Fuzzy control for gate pulse generation represented in figure 16: in this first the measured speed is converted into per unit by dividing by 3000 which is nothing but rated speed of SRM, then the error signal is obtained by subtracting with the reference i.e., 1p.u. then the obtained error signal is used as control input signals of fuzzy controller by one input is speed error and another is change in speed error. Output for the fuzzy controller is α and β, which is used to generate gate signal of 3-level converter via position sensor with the reference current of 200A. the reference current and actual current is subtracted to generate the Gate signal G_1, G_2 and G_3 this gate signal is limited by hysteresis band. Error Indices as modeled as per the equation 14-16 in frequency domain shown in figure 17.

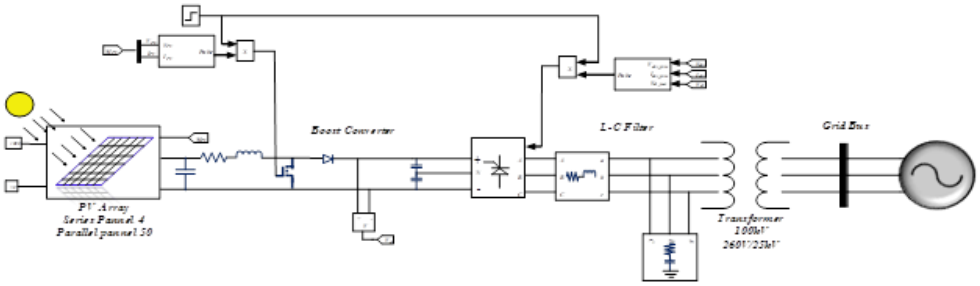

Figure 14. PV system integration with Grid

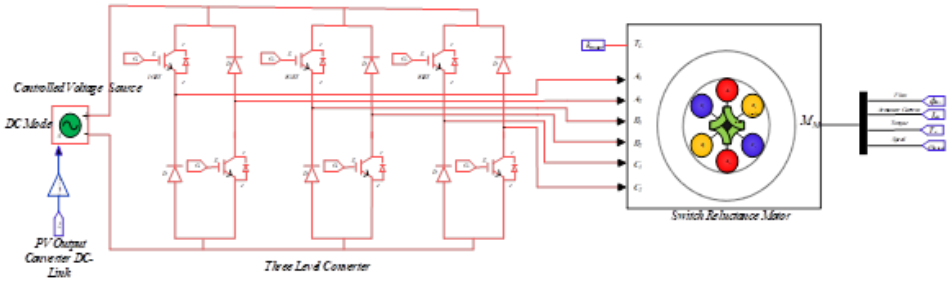

Figure 15. Three level Converter driving SRM from Controlled Voltage source

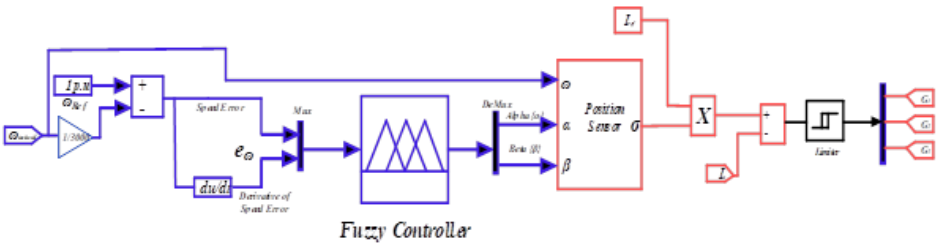

Figure 16. Modelling of Closed Loop Fuzzy control for gate pulse generation

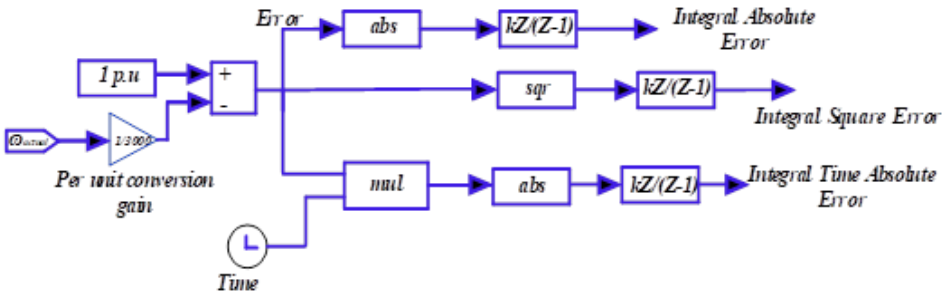

Figure 17. Modelling Error Indices

Figure 14-17 shows all are interconnected using from and goto tags; the signal attributes to corresponding lines, for easy understanding all network and control diagrams are divided into four figures.

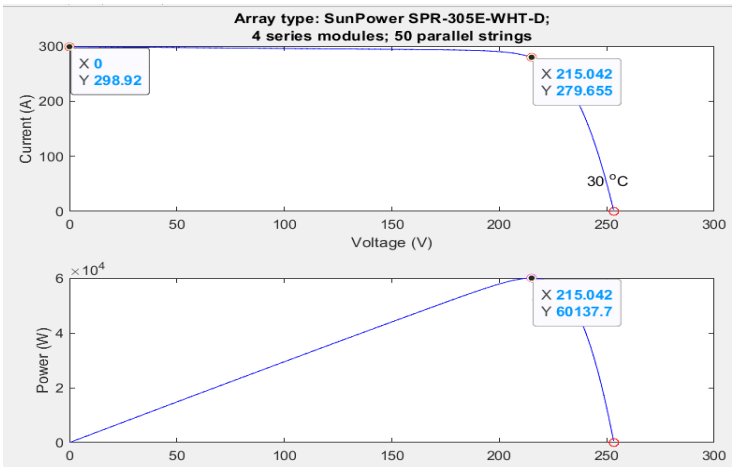

Figure 18. I-V and P-V characteristics curve of 60kw PV array

In figure 18 shows PV parameter irradiance, temperature, output power mean voltage across PV panel, duty cycle and Boost converter voltage. In our system the irradiance and temperature constant are which is of 1000w/m2 and 30 deg Celsius. PV system is designed for 60kw for that series and parallel 50 and series string of 4. The mean voltage of the PV array is of 249.9V which is a boost to dc voltage of 500V From the figure 18 we can see the voltage level and duty cycle of the boost converter, which is operating at a duty cycle of 0.5.

Figure 20 shows the SRM parameters which are flux, current, torque and speed. The characteristic of SRM is ripple in nature with respect to all parameters, so this is the reason that in the graph we can see graphs that are all ripple. The main objective of our work is to achieve desirable speed with less amount of time and the corresponding error indices. The desirable speed for our system is 3000rpm It can be noted that based on fuzzy tuning, the turn on and turnoff angle is strictly decided to get the required speed.

Figure 21 shows that the desirable speed of the SRM motor is achieved within 1.9 sec, whereas without fuzzy controller fails within that time. So, the main important thing from this graph is that controller play an important role in turn tuning of turn-on and turn-off angle matter. To pick up speed of SRM with controller is less time, hence the settling time is less. With out fuzzy controller, the turn-on and turn-off angles are between 45 deg and 75 deg. For fixed angles the motor it will take more time to achieve desirable speeds of nearly 5 seconds. Error Indices for with and without controller are plotted in figure 22.1-22.6.

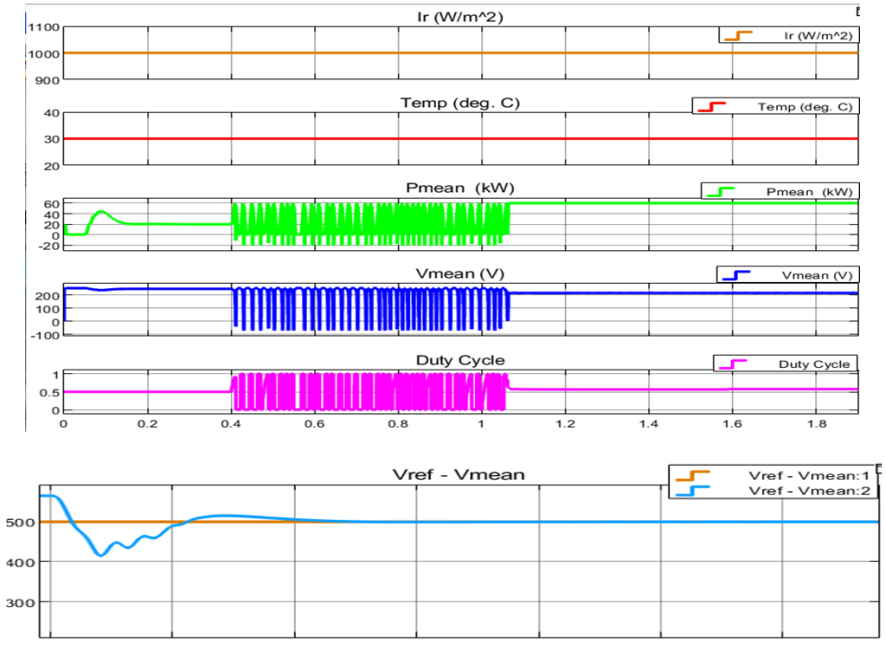

Figure 19. Measurement of PV system parameter.

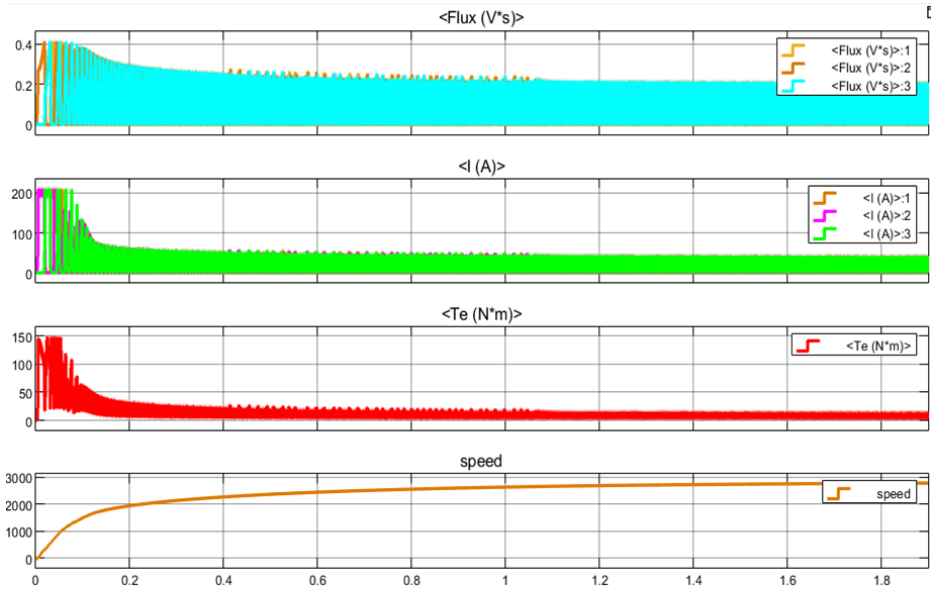

Figure 20. SRM system parameter with fuzzy controller

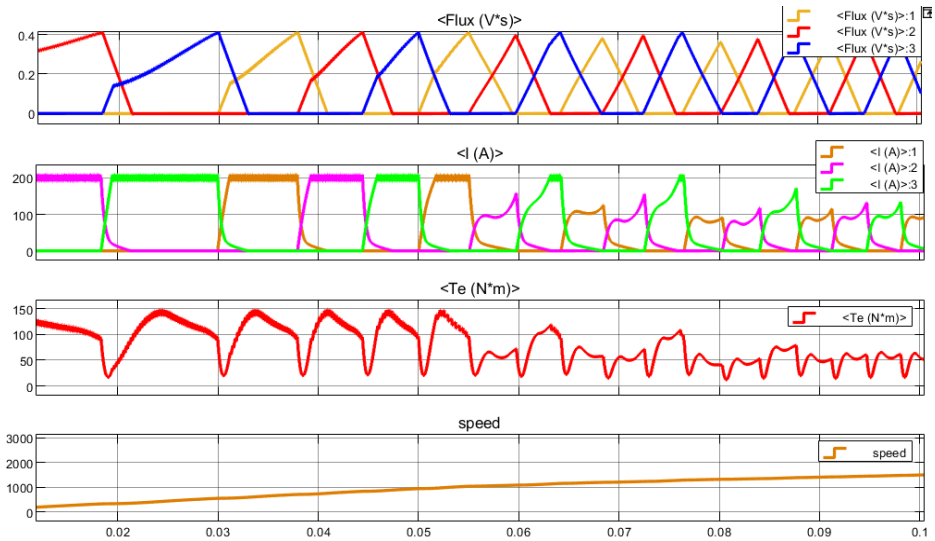

Figure 20.1. Zoom In view SRM system parameter with fuzzy controller.

Figure 20.1 is zoom in view of Figure 19 where we can see the pattern of SRM parameter.

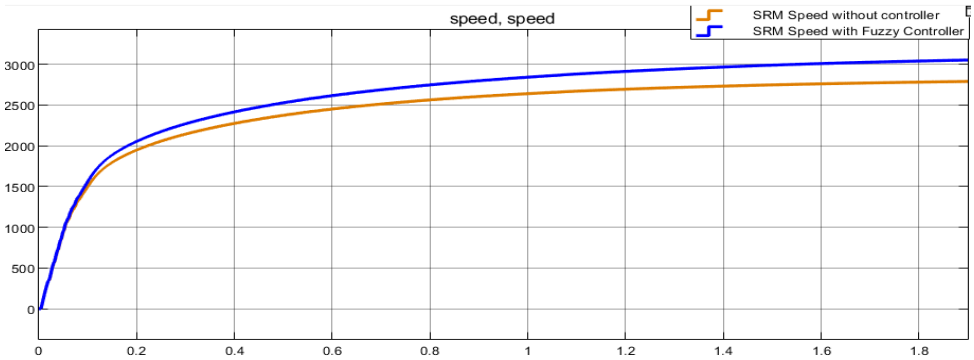

Figure 21. SRM Speed for without and with Fuzzy Controller Vs Time (Sec)

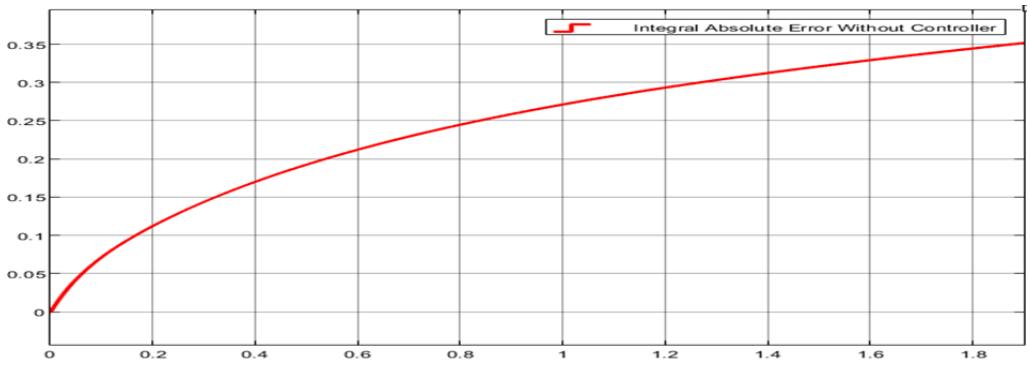

Figure 22.1. Integral Absolute Error without Controller Vs Time (Sec)

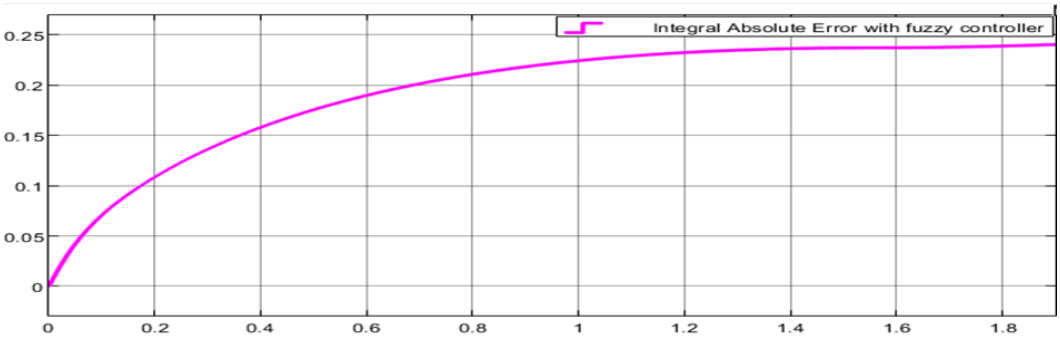

Figure 22.2. Integral Absolute Error with Fuzzy Controller Vs Time (Sec)

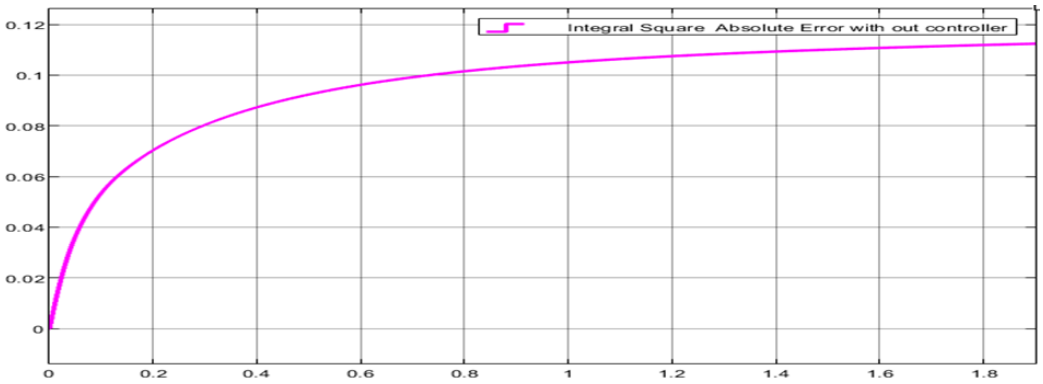

Figure 22.3. Integral Square Error without Controller Vs Time (Sec)

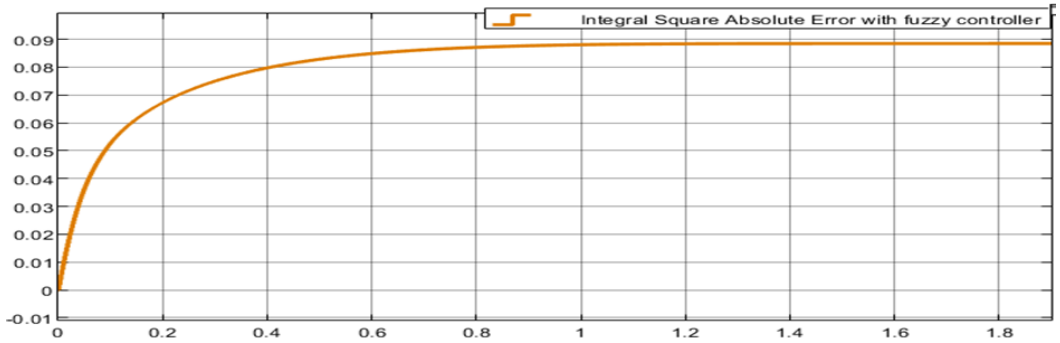

Figure 22.4. Integral Square Error with Fuzzy Controller Vs Time (Sec)

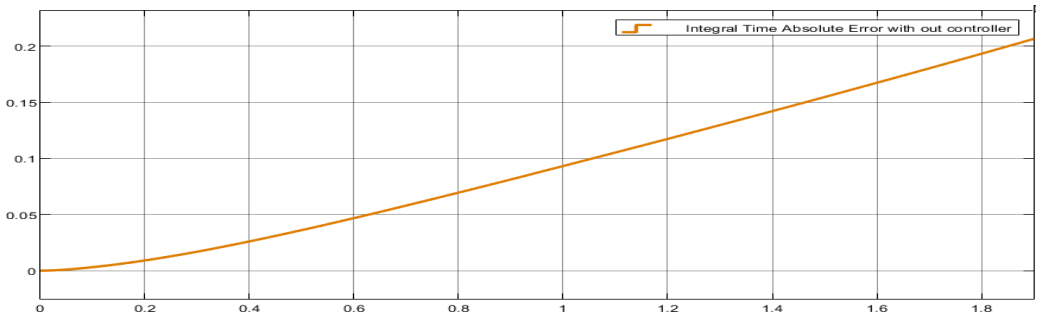

Figure 22.5. Integral Time Absolute Error without Controller Vs Time (Sec)

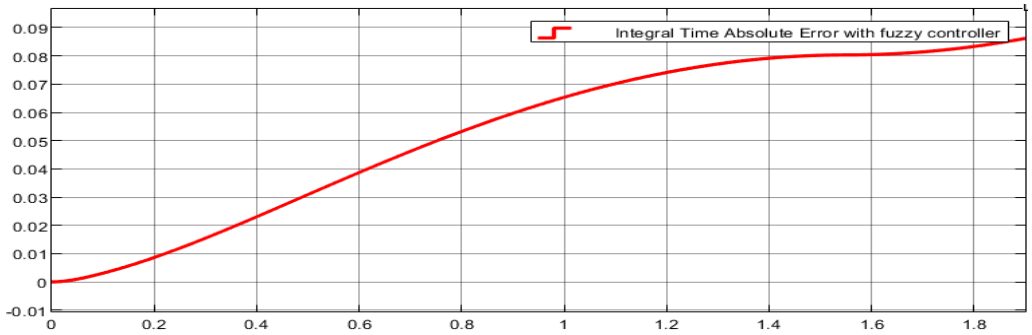

Figure 22.6. Integral Time Absolute Error with fuzzy Controller Vs Time (Sec)

Table 3. Fuzzy based optimal Tuning of Turn on and turn off angle

Sl. No	**Turn on angle**	**Turnoff angle**	**speed**
1.	43.98765	77	3031
2.	44.1	77	3012
3.	44.1	76.1	3009
4.	44.1	76.00123	3008
5.	44.1234	75.968	3003
6.	44.1234	75.8	3002
7.	44.1234	75.6	3001
8.	**44.1290**	**75.72**	**3000**
9.	44.3120	74.82	2998
10.	44.4120	74.90	2998
11.	44.5120	73.21	2996
12.	44.6120	73.11	2995
13.	44.7120	72.31	2994
14.	44.8120	72.10	2993
15.	44.9120	71.01	2990

The table show the optimal turn on and turn off angle for SRM motor the evaluation this angle is obtained by optimal fuzzy based tuning, **Sl.No. 8** give the best optimal value of turn and turn off angle for the speed for **3000 rpm**

Table 4. Comparision of Proposed and Existing work

Sl. no	Author Contribution	Parameter		
		Speed	Time(sec)	Controller
1	Kirti R chichate et.al [32]	3000	5	PID
2	Proposed	3000	**1.9**	Fuzzy based Ton-Toff angle

Table 4 shows the improvement of proposed work with existing method as we can observe from serial no.1 Kirti R chichate et.al (2020) have proposed the speed control of SRM using PID control for the reference speed of 3000 but they are end up with 2970-2980 in **5sec**.In the proposed work the reference speed is of

3000rmp and the actual speed of SRM is achieved to 3000rpm within **1.9sec** with turnon and turnoff angle of SRM based on fuzzy controller.

Table 5. Error Indices for without controller and with fuzzy controller speed Performance

SL. No	Parameter	Error Indices Without Controller	With Fuzzy Controller
1.	IAE	0.3516	**0.2405**
2.	ITAE	0.2067	**0.0862**
3.	ISE	0.1124	**0.0885**

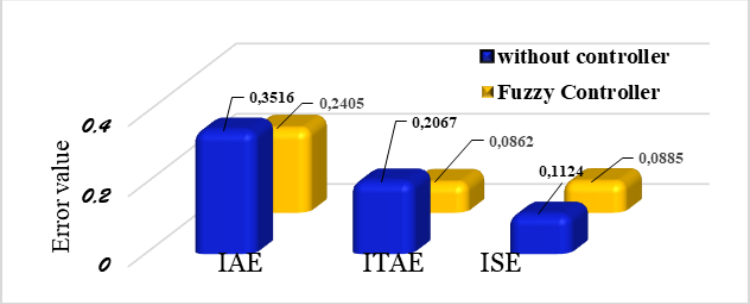

Figure 23. Error Indices for with and without Controller

In table 5 the error indices are tabulated and the corresponding graph for with and without controllers is plotted. It can observe that the IAE is reduced from 0.3516 to 0.2405, ITAE reduces from 0.2067 to 0.0862 and ISE reduces from 0.1124 to 0.0885. Figure 22 shows the error indices for both with and without controllers.

7. CONCLUSION

In this paper, novel work on Mamdani-based two-input, two-output fuzzy controller for angles of turning on and off is evaluated. Based on the closed loop response of the system for accurate speed control of SRM and the corresponding error indices ITAE, IAE, ISE for with and without controller is Analyzed and Compared. Finally, it concluded that the system responds faster with a proposed Mamdani-based fuzzy controller than without controller and existing PID controller, performance of speed control of SRM with Fuzzy Control will significantly reduced error indices.

COMPLIANCE WITH ETHICAL STANDARDS

The authors certify that they have no involvement in any organization or entity with any financial interest, or non-financial interest in the subject matter discussed in this manuscript.

REFERENCES

[1] X. Hu, J. Jiang, B. Egardt and D. Cao (2015) "Advanced Power-Source Integration in Hybrid Electric Vehicles: Multicriteria Optimization Approach," in IEEE Transactions on Industrial Electronics, vol. 62, no. 12, pp. 7847-7858, doi: 10.1109/TIE.2015.2463770.

[2] L. Dang, N. Bernard, N. Bracikowski and G. Berthiau(2017) "Design Optimization with Flux Weakening of High-Speed PMSM for Electrical Vehicle Considering the Driving Cycle," in IEEE Transactions on Industrial Electronics, vol. 64, no. 12, pp.

[3] L. Chen, G. Götting and I. Hahn(2017) "DC-Link Current and Torque Ripple Optimized Self-Sensing Control of Interior Permanent-Magnet Synchronous Machines for Hybrid and Electrical Vehicles," in IEEE Transactions on Industry Applications, vol. 53, no. 5.

[4] F. Meng, Z. Yu, Y. Chen, C. Gan and R. Qu (2019) "Development of Switched Reluctance Motor Drives with Power Factor Correction Charging Function for Electric Vehicle Application," 22nd International Conference on Electrical Machines and Systems (ICEMS), pp. 1-6, doi: 10.1109/ICEMS.2019.8922159.

[5] Omer Sajid, et.al., (2018) "Performance Analysis of Switched Reluctance Motor for 24/7 Working Environment", Smart Cities: Improving Quality of Life Using ICT & IoT (HONET-ICT) 2018 15th International Conference on, pp. 56-60.

[6] R. Krishnan, R. Arumugan and J. F. Lindsay (1998) "Design procedure for switched-reluctance motors," in IEEE Transactions on Industry Applications, vol. 24, no. 3, pp. 456-461, doi: 10.1109/28.2896.

[7] Hao Chen and Chao Zhang (2000) "A three-phase 6/8 structure switched reluctance motor drive," PowerCon 2000. 2000 International Conference on Power System Technology. Proceedings (Cat. No.00EX409), pp. 195-200 vol.1, doi: 10.1109/ICPST.2000.900055.

[8] J. F. Pan, Y. Zou and G. Cao (2013) "An Asymmetric Linear Switched Reluctance Motor," in IEEE Transactions on Energy Conversion, vol. 28, no. 2, pp. 444-451, doi: 10.1109/TEC.2013.2252178.
[9] M. N. Anwar, I. Husain and A. V. Radun (2001) "A comprehensive design methodology for switched reluctance machines," in IEEE Transactions on Industry Applications, vol. 37, no. 6, pp. 1684-1692, Nov.-Dec. 2001, doi: 10.1109/28.968179.
[10] H. Chen, X. Wang, J. J. Gu and Q. Song (2010) "Simulation on parallel drive system of double Switched Reluctance motors based on sliding mode & fuzzy controllers," 2010 IEEE Electrical Power & Energy Conference, pp. 1-5, doi: 10.1109/EPEC.2010.5697237.
[11] C. M. Stephens, et.al., (1991) "Fault detection and management system for fault-tolerant switched reluctance motor drives," in IEEE Transactions on Industry Applications, vol. 27, no. 6, pp. 1098-1102, Nov.-Dec, doi: 10.1109/28.108460.
[12] V. P. Vujicic. (2012). Minimization of Torque Ripple and Copper Losses in Switched Reluctance Drive. IEEE Transactions on Power Electronics, 27, 388-399.
[13] Oshaba, A.S., Ali, E.S. & Abd Elazim, S.M (2017) PI controller design for MPPT of photovoltaic system supplying SRM via BAT search algorithm. Neural Comput & Applic 28, 651–667. https://doi.org/10.1007/s00521-015-2091-9
[14] W. Cao, B. C. Mecrow, G. J. Atkinson, J. W. Bennett and D. J. Atkinson (2012) "Overview of Electric Motor Technologies Used for More Electric Aircraft (MEA)," in IEEE Transactions on Industrial Electronics, vol. 59, no. 9, pp. 3523-3531, Sept, doi: 10.1109/TIE.2011.2165453.
[15] K. M. Rahman and M. Ehsani (1996) "Performance analysis of electric motor drives for electric and hybrid electric vehicle applications," Power Electronics in Transportation, pp. 49-56, doi: 10.1109/PET.1996.565909.
[16] Husain, et.al., (2002) "Minimization of torque ripple in SRM drives," in IEEE Transactions on Industrial Electronics, vol. 49, no. 1, pp. 28-39, Feb, doi: 10.1109/41.982245.
[17] Jessi Sahaya Shanthi, L., Arumugam, R. & Taly, Y.K. (2012) A novel rotor position estimation approach for an 8/6 solid rotor switched reluctance motor. Neural Comput & Applic 21, 461–468. https://doi.org/10.1007/s00521-010-0447-8
[18] C. Gan, J. Wu, Q. Sun, W. Kong, H. Li and Y. Hu (2018) "A Review on Machine Topologies and Control Techniques for Low-Noise Switched Reluctance Motors in Electric Vehicle Applications," in IEEE Access, vol. 6, pp. 31430-31443, doi: 10.1109/ACCESS.2018.2837111.
[19] M. Polat, A. Yildiz (2020) "Influence of Different Pole Head Shapes on Motor Performance in Switched Reluctance Motors," Advances in Electrical and Computer Engineering, vol.20, no.3, pp.75-82, doi:10.4316/AECE.2020.03009.
[20] El-Hay, E.A., El-Hameed, M.A. & El-Fergany, A.A (2019) Improved performance of PEM fuel cells stack feeding switched reluctance motor using multi-objective dragonfly optimizer. Neural Comput & Applic 31, 6909–6924. https://doi.org/10.1007/s00521-018-3524-z
[21] Ashwin Raj, P. K. Sreekanth (2017) "Modelling and simulation of SRM based automatic transmission system for hybrid vehicles in Ansys Maxwell", Circuit Power and Computing Technologies (ICCPCT) 2017 International Conference on, pp. 1-6.
[22] Alrifai Muthana, Zribi Mohamed, Rayan Mohamed, R. Krishnan (2010) “Speed control of switched reluctance motors taking into account mutual inductances and magnetic saturation effects” 5110.1016/j.enconman.2010.01.004 Energy Conversion and Management.
[23] Kalaivani.L. Perumal, Subburaj Mariasiluvairaj, Willjuice Iruthayarajan (2013) Speed control of switched reluctance motor with torque ripple reduction using non-dominated sorting genetic algorithm (NSGA-II) 53 10.1016/j.ijepes.2013.04.005 International Journal of Electrical Power & Energy Systems
[24] M. Rodrigues, P. J. Costa Branco and W. Suemitsu (2001) "Fuzzy logic torque ripple reduction by turn-off angle compensation for switched reluctance motors," in IEEE Transactions on Industrial Electronics, vol. 48, no. 3, pp. 711-715, June, doi: 10.1109/41.925598.
[25] Saha, Nutan Panda, A.K.Panda, Sidhartha (2016) “Speed control with torque ripple reduction of switched reluctance motor by many optimizing liaison technique”, Journal of Electrical Systems and Information Technology https://doi.org/10.1016/j.jesit.2016.12.013.
[26] K. R. Chichate, S. R. Gore and A. Zadey (2020) "Modelling and Simulation of Switched Reluctance Motor for Speed Control Applications," 2020 2nd International Conference on Innovative Mechanisms for Industry Applications doi: 10.1109/ICIMIA48430.2020.9074845.
[27] Tariq, Iqra, Muzzammel, Raheel,et.al., (2020) ”Artificial Neural Network-Based Control of Switched Reluctance Motor for Torque Ripple Reduction” , 1024-123X, Mathematical Problems in Engineering, Hindawi.
[28] M. Rodrigues da Cunha Reis, W. R. H. de Araújo, W. P. Calixto and A. J. Alves (2015) "Analysis of switched reluctance motor efficiency under different speed control strategies," 2015 CHILEAN Conference on Electrical, Electronics Engineering, Information and Communication Technologies doi: 10.1109/Chilecon.2015.7400419.
[29] K. K. Nimisha and R. Senthilkumar (2018) "Optimal Tuning of PID Controller For Switched Reluctance Motor Speed Control Using Particle Swarm Optimization," 2018 International Conference on Control, Power, Communication and Computing Technologies (ICCPCCT), pp. 487-491, doi: 10.1109/ICCPCCT.2018.8574234.
[30] Oshaba, A.S., Ali, E.S. & Abd Elazim, S.M (2017) Speed control of SRM supplied by photovoltaic system via ant colony optimization algorithm. Neural Comput & Applic 28, 365–374.

[31] Krishnan, Ramu. Switched reluctance motor drives: modeling, simulation, analysis, design, and applications. CRC press, 2017.
[32] K. R. Chichate, S. R. Gore and A. Zadey, "Modelling and Simulation of Switched Reluctance Motor for Speed

APPENDIX

Control Applications," 2020 2nd International Conference on Innovative Mechanisms for Industry

Appendix Terminology

R_s per phase resistance
λ per phase flux linkage
V Per Phase Voltage
e Induced Electromotive force(emf)
K_b emf constant
L inductance dependent on the position of the rotor
P_i Instantaneous input power
i Instantaneous DC current
ω_m *Rotor speed (rad sec)*
∅ Rotor position (rad)
P_a Air gap Power
P differential operator
t Time
T_e Electromagnetic Torque
e_ω speed error in per unit
$\omega_{ref_{p.u}}$ reference speed in per unit i.e., is 1 p.u
$\omega_{act_{p.u}}$ actual speed in per unit
α Turn on angle
β Turn off angle

Simulation Parameters of SRM

Sl.no	Parameter	Ratings
1.	Power	60kW
2.	Speed	3000RPM
3.	DC Link Voltage	120V
4.	Stator Resistance	0.05
5.	Stator Pole Arc	32
6.	N_{rotor}	4
7.	N_{stator}	6

BIOGRAPHY OF AUTHORS

M. Naveen Kumar received, B.Tech., M. Tech from Electrical and Electronics Department, Jawaharlal Nehru Technological University Hyderabad in 2016 and 2019, respectively. Currently pursuing 3nd year full time Ph. D in Electrical and Electronics Department at The National Institute of Engineering, Mysore, Karnataka, India under Visvesvaraya Technological University Belgaum. Area of research in Battery Management System on Electric Vehicles Integration in Electric Power System.

Dr. R. Chidanandappa received Bachelor of Engineering degree from Kuvempu University, M. Tech and Ph. D from Visvesvaraya Technological University Belgaum. Currently working as an Associate Professor in the Dept. of Electrical and Electronics Engineering at The National Institute of Engineering, Mysore, Karnataka, India. Research interest is in Distribution automation, Smart grid with Power electronics control and Power quality problems and also quite interested in Electric vehicle integration to grid with battery storage application. Currently working on a project titled "Establishment of real time monitoring system R&D facility for efficient operation of campus power distribution network", Sponsored by VGST, and Govt. of Karnataka". At present guiding one full time Ph. D scholar (AICTE-NDF Scheme) in area of Battery Management System on Electric vehicles.